

Laser sintering of copper nanoparticles on top of silicon substrates

A Soltani¹, B Khorramdel Vahed¹, A Mardoukhi² and M Mäntysalo¹

¹Department of Electronics and Communication Engineering, Tampere University of Technology, Tampere, 3720, Finland

²Department of Material Science, Tampere University of Technology, Tampere, 33720, Finland

E-mail: ayat.soltani@tut.fi

Received 2 June 2015, revised 10 November 2015

Accepted for publication 13 November 2015

Published 9 December 2015



CrossMark

Abstract

This study examines the sintering of inkjet printed nanoparticle copper ink in a room environment using a laser as a high speed sintering method. Printed patterns were sintered with increasing laser scanning speed up to 400 mm s^{-1} . The resistivities of the sintered structures were measured and plotted against the scanning speeds. Increased resistivity seems to correlate with increased scanning speed. A selection of analytical methods was used to study the differences in microstructure and composition of the sintered structures. Based on the results, no discernable difference in the microstructure was noticed between the structures sintered using 20 mm s^{-1} to 400 mm s^{-1} scanning speeds; only the structure scanned using 5 mm s^{-1} speed showed a vastly different microstructure and no resistivity was measurable on this structure. Compositional studies revealed that, apart from the structure scanned with 5 mm s^{-1} speed which contained the highest oxygen, the rest of the structures showed a steady oxygen increase with increased scanning speed.

Keywords: Inkjet, sintering, resistance, nanoparticles

(Some figures may appear in colour only in the online journal)

Introduction

Printed electronics as a flexible and convenient manufacturing method has gained a strong foothold in the current electronic packaging field. The advent of nanoparticle technology has paved the way for the production of inks suitable for inkjet printing technology that contain various nanoparticle metals (gold (Au), silver (Ag), copper (Cu)). These metallic nanoparticles are suspended in some form of liquid (such as water and toluene) containing additives such as dispersants and adhesion promoters. In some cases, the particles are coated with a polymer to protect the particles from oxidation. While the small size of nanoparticles gives these metallic inks the ability to be inkjetted, it also provides another useful property: the melting point of nanoparticles of a particular metal is

lower than the bulk material [1, 2]. This lower melting point enables the sintering of such materials at a much lower temperature compared to the bulk material, possibly reducing the cost of the sintering process and enabling applicability to large areas.

Various sintering methods have been extensively studied for a variety of nanoparticle inks; these methods include plasma [3], rapid electrical sintering [4], and intense pulsed light (IPL) sintering [5]. In the case of non-reactive metals such as Au and Ag, sintering is possible by simply heating up the printed ink in an oven [6, 7]. However, oven sintering can be time-consuming and costly. For this reason, other forms of sintering have been explored. Examples of cost efficient and high speed sintering methods are laser and IPL sintering. While laser sintering relies on the ability of nanoparticles to absorb energy from a continuous or pulsed laser source, in IPL sintering the energy is provided by a set of strong xenon lamps. These methods have been previously studied on various substrates, such as Au on silicon (Si) wafer [8] and glass [9], Ag on glass [10] and polyimide [11].



Content from this work may be used under the terms of the Creative Commons Attribution 3.0 licence. Any further distribution of this work must maintain attribution to the author(s) and the title of the work, journal citation and DOI.

Table 1. Printing parameters.

Ink	CI-002, Intrinsic Cu
Particle size	50 nm
Solid content	25 wt. %
Printing speed	100 mm s ⁻¹
Printing distance	1.0 mm
Printing plate temperature	50 °C
Printhead	Dimatix Spectra SE-128
Printing voltage	80 V
Printhead temperature	55 °C
Drop volume	30 pl
Drop diameter on substrate	40 μm
Print resolution	900 dpi

Although Ag and Au provide excellent conductivity, their relatively high price limits their application in the field of inkjet printed electronics. Since the main goal of using inkjet printed electronics is cost reduction in the manufacturing of electronics, the demand is high for nanoparticle printable inks with lower cost that can provide electrical properties similar to Au and Ag. One potential candidate for such requirement is Cu [12, 13]. However, due to high reactivity, Cu oxidation rate increases exponentially with increasing temperature in an ambient environment [14]. Consequently, the sintering process for this particular metallic ink has to be carried out in an inert environment. This requirement defeats the purpose of using Cu ink as it will increase the processing costs.

Processes that provide high amounts of concentrated energy in a relatively small time window are suitable for sintering of Cu nanoparticles. In such sintering methods, the Cu nanoparticles do not have enough time to oxidate. Various high speed sintering methods have been researched on Cu nanoparticle inks, such as IPL [15] and laser sintering [16]. A comparison of laser and IPL sintering for printed Cu on top of plastics is presented in [17]. However, until now most of these studies have been focused on sintering printed Cu nanoparticle inks on top of substrates such as glass and polyimide. Usage of Si as a substrate also needs attention in order to enable the breakout of inkjet technology in the semiconductor fabrication process.

It should be noted that sintering of Cu nanoparticle ink on Si substrates is more demanding as demonstrated in a simulation by Niittynen *et al* [18], mostly because the heat conductance of Si is rather high. For example, the heat conductivity of Si is 149 W m⁻¹ K⁻¹ compared to heat conductivity of polyimide which is 0.12 W m⁻¹ K⁻¹. Thus, Si substrate acts like a heat-sink while dissipating the heat coming from the energy source. For this reason, the maximum temperature reachable is much lower for Si compared to polyimide using the same power [18]. On the other hand, Si can withstand high temperatures unlike polyethylene terephthalate (PET) and polyimide substrates. This research aims to study the effect of laser scanning speed on the sheet resistance of the sintered Cu structure on top of Si wafers. The microstructure and composition of the sintered structures are analyzed and related to the measured sheet resistance values.

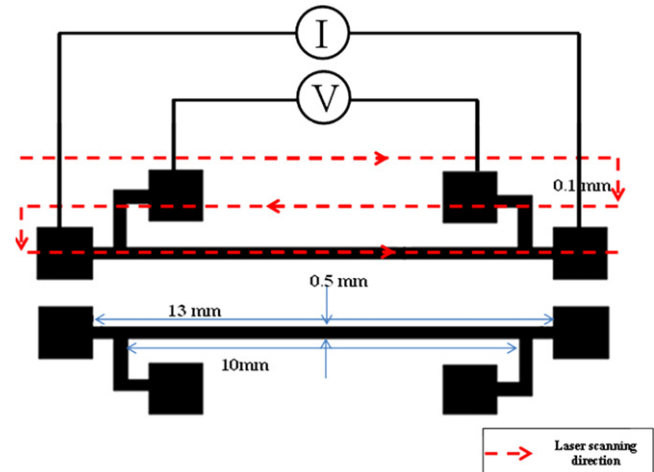


Figure 1. Four-point pattern and demonstration of laser scanning pattern over the printed pattern. The laser was moved in 0.1 mm steps to cover the entire pattern.

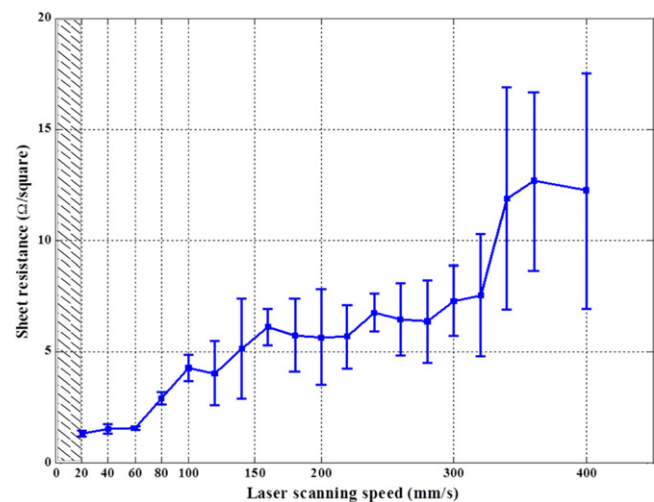


Figure 2. Sheet resistance values versus laser scanning speed.

Experiment

The ink used in this study is a commercially available Cu nanoparticle ink, CI-002 containing nanoparticles with around 50 nm diameter (solid content of 25 wt. %). The particles are coated with an organic polymer in order to prevent agglomeration as well as to ensure a long shelf life. The printer setup used was an iTi XY MDS2.0 inkjet printer using a drop on demand print-head Dimatix Spectra SE-128 comprised of 128 nozzles producing 30 pl droplets. The substrate is a 6 inch Si wafer with 2.55 μm thick oxide layer on top. Prior to the printing, the Si substrates were cleaned by wiping with isopropanol and heated up to 50 °C. After printing, the printed structures were left overnight at room temperature to completely dry. Printing parameters are presented in table 1.

The printed patterns were sintered using an 808 nm continuous wave semiconductor laser HLU35C10 × 2-808-CD by Lissotchenko Mikro-optik (Limo). For optimum sintering, the longer edge of the laser spot was placed parallel to

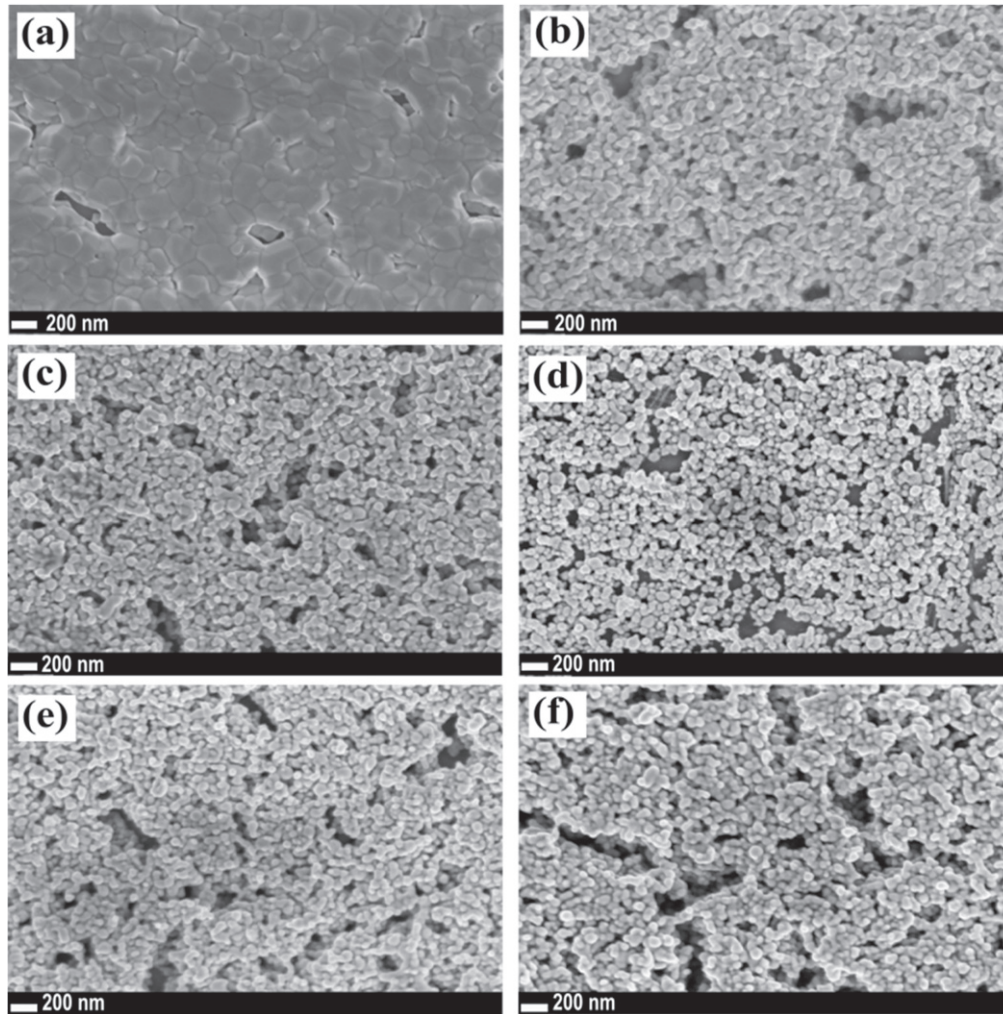


Figure 3. SEM pictures of sintered Cu structures with various scanning speeds (a) 5 mm s^{-1} (b) 20 mm s^{-1} (c) 100 mm s^{-1} (d) 200 mm s^{-1} (e) 300 mm s^{-1} (f) 400 mm s^{-1} .

the sintering direction. The custom made laser diode along with the cooling unit is placed face down on top of the focusing lens. Instead of moving the laser diode over the substrate, a motorized table was used to move the substrate under the laser spot. This table is able to move in X and Y directions with various speeds. A stepwise scanning pattern with a power of 20 W was used to ensure the uniform sintering of the entire surface of the printed patterns, as presented in figure 1. Each step was 0.1 mm , which is smaller than the diameter of the laser spot ($\sim 0.2 \text{ mm}$). This allows each step in the movement in the X direction to be superimposed on the previous step, guaranteeing that no point on the pattern is left untouched by the laser.

Resistance was measured using a Keithley 2400 multi-meter on a four-point structure shown in figure 1. The microstructure of the sintered samples was studied by a field emission Zeiss Ultra-55 scanning electron microscope (SEM). Composition of the sintered patterns was examined by x-ray diffraction (XRD) and Zeiss ULTRA plus energy-dispersive spectroscopy (EDS).

Results and discussion

Five test structures were scanned using a laser with various power outputs (1 to 20 W) in order to determine the optimum power value. Based on this initial step, the power output of 20 W was chosen. The measured sheet resistance values using this laser power output are presented in figure 2 for various scanning speeds from 20 mm s^{-1} to 400 mm s^{-1} . Each point represents three measurements from three different samples. No resistance was measurable for scanning speeds lower than 20 mm s^{-1} .

Figure 2 shows that the sheet resistance increases slowly up to 60 mm s^{-1} and at a faster rate from 60 mm s^{-1} to 100 mm s^{-1} where a slight decrease is noticed before it increases again. This erratic behavior is observed throughout the graph but overall an increasing trend is noticeable in the sheet resistance values. However, the range of sheet resistance increases along the sheet resistance value, especially for scanning speeds above 100 mm s^{-1} . On the surface the reason for the increased resistivity values seems to be that the laser

Table 2. Oxygen levels of sintered structures scanned with various speeds.

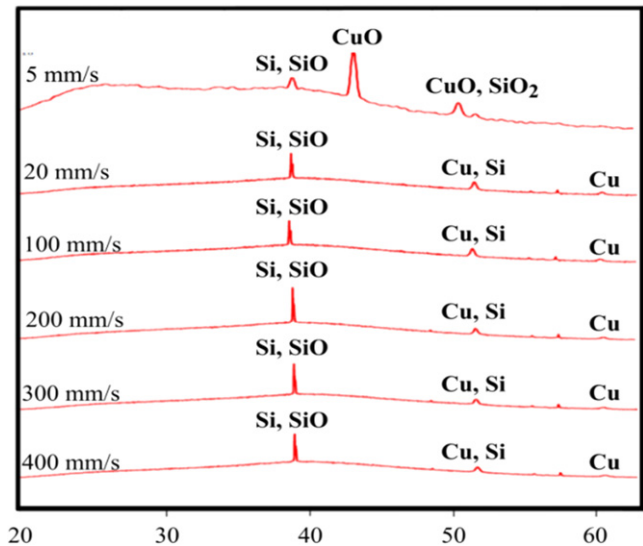
Scanning speed	Oxygen wt. %	Sheet resistance Ω/square
5 mm s^{-1}	22.8%	—
20 mm s^{-1}	1.98%	1.321
100 mm s^{-1}	1.88%	4.28
200 mm s^{-1}	3.6%	5.63
300 mm s^{-1}	11.4%	7.29
400 mm s^{-1}	12.22%	12.233

dwel time on the samples is decreased with increased scanning speed. Consequently, less heat generated by the laser is transferred to the printed patterns. Figure 3 shows the SEM pictures of the samples sintered with scanning speeds of 5 mm s^{-1} , 20 mm s^{-1} , 100 mm s^{-1} , 200 mm s^{-1} , 300 mm s^{-1} and 400 mm s^{-1} .

Comparing all of the six samples reveals that the structure scanned with a slow speed of 5 mm s^{-1} (figure 3(a)) is vastly different from the other structures. Unlike the figures 3(b) to (f), no individual particles are discernable in the microstructure of figure 3(a); hence it seems that the heat coming from the laser is too great to facilitate proper sintering. Keeping in mind that the sintering process is compacting and forms a solid mass of material *without* melting the particles, it is probable that the particles have melted in figure 3(a). In this sample, small ‘islands’ are seen which are connected to each other on their boundaries instead of individual particles. Another interesting observation made from studying the SEM pictures is how the microstructures of samples scanned with speeds of 20 mm s^{-1} and higher are virtually indistinguishable. In these samples, individual particles are readily discernable and they have retained their spherical shapes. These particles have been properly sintered and connected on the surface, thus forming a conductive path throughout the structure. A common feature of the sintered samples is the presence of elongated microvoids throughout the structures. Looking at figure 3, these microvoids are present in all of the structures regardless of the scanning speed and their density does not seem to vary much from one sample to the other.

Furthermore, EDS tests were conducted to explore any possible difference in the composition of the samples. Table 2 shows the amount of oxygen detected in each of the structures that were discussed in figure 3.

The percent of oxygen weight detected is more or less the same for speeds 20 mm s^{-1} and 100 mm s^{-1} , while it rises slightly when the scanning speed is increased to 200 mm s^{-1} . This correlates to the resistivity shown in figure 2. The amount of detected oxygen increases by more than five times when the scanning speed is increased to 300 mm s^{-1} . The highest oxygen amount however, belongs to the sample scanned with 5 mm s^{-1} speed. When the printed structure is sintered with less than 20 mm s^{-1} laser scanning speed, the heat transferred to the sample is very high over a longer period of time. This will lead to oxidation of Cu nanoparticles since they have more time to react with oxygen.

**Figure 4.** XRD patterns of sintered Cu structures.

As the final step in the study, XRD measurements of the samples given in table 2 will be discussed. As shown in figure 4, no obvious differences are noticed by comparing the XRD results of the samples scanned with velocities of 20 mm s^{-1} , 100 mm s^{-1} , 200 mm s^{-1} , 300 mm s^{-1} and 400 mm s^{-1} . Similar to previous results, the sample sintered with 5 mm s^{-1} scanning speed is the only sample that shows obvious differences from the rest of the samples. The XRD graph for this sample shows clear peaks belonging to Cu oxide. By combining the data in table 2 and the results from the XRD graphs, it can be concluded that for the sample sintered using 5 mm s^{-1} speed, the amount of oxygen in the structure is very high and detectable by x-ray. The rest of the samples, however, have a much smaller oxygen amount that is virtually undetectable by x-ray. This is likely related to the Si substrate as it will block the detection of small traces of oxygen in the structure. It can be deduced that there is some Cu oxide present in all of the structures, but it is not high enough to hinder the conductivity of samples scanned with velocities 20 mm s^{-1} and higher, at least not as much as for the 5 mm s^{-1} case.

Conclusion

In this research, sintering of inkjet printed Cu nanoparticles on top of a Si substrate was demonstrated. Based on the initial results, a laser seems to be a good alternative to more traditional sintering methods such as oven sintering. Very low scanning speeds (under 20 mm s^{-1}) will lead to oxidation of the printed structures where the sintering time frame is too high to facilitate proper sintering, leading to oxidation of Cu nanoparticles. Increasing the scanning speed of the laser fixes this problem. However, there seems to be a threshold after which the measured sheet resistance starts to increase with increasing scanning speed. Based on the EDS and XRD results, this increase in the sheet resistance is connected to the increase in oxygen present in the sintered structures.

Acknowledgments

This work is supported by ENIAC-JU Project Prominent grant No. 324189 and Tekes grant No. 40336/12. MM is supported by Academy of Finland grant no. 288945.

References

- [1] Lai S L, Guo J Y, Petrova V, Ramanath G and Allen L H 1996 Size-dependent melting properties of small tin particles: nanocalorimetric measurements *Phys. Rev. Lett.* **77** 99–102
- [2] Safaei A, Shandiz M A, Sanjabi S and Barber Z H 2007 Modelling the size effect on the melting temperature of nanoparticles, nanowires and nanofilms *J. Phys.: Condens. Matter.* **19** 216216
- [3] Reinhold I, Hendriks C E, Eckardt R, Kranenburg J M, Perelaer J, Reinhard R B and Ulrich S S 2009 Argon plasma sintering of inkjet printed silver tracks on polymer substrates *J. Mater. Chem.* **19** 3384–8
- [4] Allen M L, Aronniemi M, Mattila T, Alastalo A, Ojanpera K, Suhonen M and Seppa H 2008 Electrical sintering of nanoparticle structures *Nanotechnology* **19** 175201–5
- [5] Dharmadasa R, Jha M, Delaina A A and Druffel T 2013 Room temperature synthesis of a copper ink for the intense pulsed light sintering of conductive copper films *ACS Appl. Mater. Interfaces* **5** 13227–34
- [6] Halonen E, Viiru T, Ostman K, Cabezas A and Mantysalo M 2013 Oven sintering process optimization for inkjet-printed Ag nanoparticle ink *IEEE Trans. Compon. Packag. Manuf. Technol.* **3** 350–6
- [7] Bakhashev T and Subramanian V 2009 Investigation of gold nanoparticle inks for low-temperature lead-free packaging technology *J. Electron. Mater.* **38** 2720–5
- [8] Ko H S, Pan H, Grigoropoulos C P, Lucombe C K, Frechet J M J and Poulikakos D 2007 Air stable high resolution organic transistors by selective laser sintering of ink-jet printed metal nanoparticles *Appl. Phys. Lett.* **90** 141103
- [9] Chung J, Ko S, Bieri N R, Grigoropoulos C P and Poulikakos D 2004 Conductor microstructures by laser curing of printed gold nanoparticle ink *Appl. Phys. Lett.* **84** 801–3
- [10] Peng P, Hu A and Zhou Y 2012 Laser sintering of silver nanoparticle thin films: microstructure and optical properties *Appl. Phys. A* **108** 685–91
- [11] Auyeung C R, Kim H, Matthews S A and Pique A 2007 Laser direct-write of metallic nanoparticle inks *J. Laser Micro/Nanoeng.* **2** 21–5
- [12] Leuchinger N A, Athanassiou E K and Stark W J 2008 Graphene-stabilized copper nanoparticles as an air-stable substitute for silver and gold in low-cost ink-jet printable electronics *Nanotechnology* **19** 445201
- [13] Park B K, Kim D, Jeong S, Moon J and Kim J S 2007 Direct writing of copper conductive patterns by ink-jet printing *Thin Solid Films* **515** 7706–11
- [14] Wan Y, Wang X, Hong S, Yanbo L, Ke Z and Yuhou W 2012 Corrosion behavior of copper at elevated temperature *Int. J. Electrochem. Sci.* **7** 7902–14
- [15] Lim S, Joyce M, Fleming P D, Aijazi A T and Atashbar M 2013 Inkjet printing and sintering of nano-copper ink *J. Imaging Sci. Technol.* **57** 050506
- [16] Zenou M, Ermak O, Saar A and Kotler Z 2014 Laser sintering of copper nanoparticles *J. Phys. D: Appl. Phys.* **47** 025501–12
- [17] Niittynen J, Sowade E, Kang H and Baumann R R 2015 Comparison of laser and intense pulsed light sintering (IPL) for inkjet-printed copper nanoparticle layers *Sci. Rep.* **5** 8832
- [18] Niittynen J and Mäntysalo M 2014 Testing, Characterization of Laser Sintering of Copper Nanoparticle Ink by FEM and Experimental *IEEE Trans. Compon. Packag. Manuf. Technol.* **4** 2018–25